

Analysis of the metering performance for typical shape maize seeds using DEM

Linrong Shi, Wuyun Zhao, Wei Sun*, Xiaoping Yang, Guanping Wang, Shanglong Xin

(College of Mechanical and Electrical Engineering, Gansu Agricultural University, Lanzhou 730070, China)

Abstract: The irregular shape, varying internal compositions, and uneven distributions of maize seeds can degrade the metering performance of maize seeders. This study investigates the effect of irregular maize on the performance of a high-filling-rate seed metering device using DEM. The results show that the seed population in the seed box formed large and small cycles of seed transport due to the disturbances caused by the three wheels. The increasing angular speed of the three wheels reduced the rate of seed filling in the seed filling regions by gravity and disturbances. In addition, an analysis of the repose angle formed by the dropped seed indicated that the angular speed of the taking seed wheel has a certain effect. The large angular speed reduced the coefficient of variation of the seed drop location. The repose angle of the horse tooth seed was greater than those of the other. Meanwhile, the irregular maize seed can also reduce the coefficient of variation of the seed drop location. A comparison between the simulation and experiment results indicates the number of metering seed were basically the same.

Keywords: maize seeds, seed metering performance, DEM, verification

DOI: 10.25165/j.ijabe.20231601.6813

Citation: Shi L R, Zhao W Y, Sun W, Yang X P, Wang G P, Xin S L. Analysis of the metering performance for typical shape maize seeds using DEM. *Int J Agric & Biol Eng*, 2023; 16(1): 26–35.

1 Introduction

A seed metering device is the core component of a planter. The performance determines the planter's quality. Mechanical seed metering devices are widely employed due to their simple, stable, and reliable construction. Its processes performed can be classified into seed filling, seed cleaning, seed transporting, seed metering, etc.^[1] As a contact, friction, collision, and other forms of interaction force between the seeds are subject to complex forces, the force can affect the metering quality. It is difficult to study seed metering using the continuous mechanics method. In addition, the traditional experimental method is heavily dependent on the experience of the experimenter. The discrete element method (DEM) is a numerical simulation technique used to solve problems related to discontinuous materials, including the interaction between bulk materials and the parts of agricultural parts, as well as the flow of bulk agricultural materials. Also, this technique was also used to optimize the structure of the seeder^[2,3]. The reliability of the DEM simulation model and in particular, the simulation parameters have a large impact on the results. The simulation parameters include the intrinsic and contact parameters. The intrinsic parameters consist of Poisson's ratio, density, shear

modulus, et al, which were determined through experiments. The contact parameters refer to the coefficients of recovery, static friction, and rolling friction. The shape, size, and center of mass error between the actual and simulation seed lead to the simulation distortion^[4,5]. The ideally shaped particles with varying coefficients of rolling friction and the shape particles are simulated through stacking, observing that the particle shape and coefficient of rolling friction had similar effects on the motion of the particle population, yet the shape also resisted their motion and rolling^[6]. The effects of different particle properties, particularly, shape and size, on the segregation of cohesionless materials were investigated, founding that the size and shape of the particle affected the calibration results^[7]. Maize modeling and parameter calibration must be studied separately to develop a reliable maize model. The coefficient of rolling friction is an important contact parameter^[8,9]. The parameters are indirectly obtained by approximating the experimental repose angle after gradually varying the coefficient of the rolling friction of the maize model^[10]. The maize model was established by using accurate 3D scanning technology^[11].

Nowadays, the coefficients of static friction and rolling friction were predicted through a unified regression model, which provided a reference for the prediction of the coefficient of rolling friction of irregular maize^[12]. Also, the effects of maize seed gravity center on the performance of the metering device and seeds flow were briefly discussed^[13]. For these reasons, a method to calibrate the coefficient of rolling friction for different shape types of maize seeds was proposed in this study^[14]. To further verify the feasibility of the above method, a seed metering simulation experiment was conducted using a high-filling rate maize seed metering device. The effects of the angular speed of the taking seed wheel and three shape types of maize on the taking seed number and repose angle were investigated in-depth.

2 Materials and method

2.1 Maize model

As maize seed shape and size determine the structure and

Received date: 2021-06-13 **Accepted date:** 2022-06-07

Biographies: **Linrong Shi**, PhD, Associate Professor, research interest: key technologies and equipment for precision seeding in northwest cold and arid zone, Email: shilr@gsau.edu.cn; **Wuyun Zhao**, PhD, Professor, research interest: crop production equipment project in northern dry zone, Email: zhaowuy@gsau.edu.cn; **Xiaoping Yang**, Associate Professor, research interest: agricultural mechanization engineering, Email: yangxp@gsau.edu.cn; **Guanping Wang**, PhD, Professor, research interest: agricultural electrification and automation, Email: wangguanping@gsau.edu.cn; **Shanglong Xin**, PhD, Lecturer, research interest: agricultural mechanization engineering, Email: xinshl@126.com.

***Corresponding author:** **Wei Sun**, PhD, Professor, research interest: agricultural mechanization engineering. Mechanical and Electrical Engineering College, Gansu Agricultural University, Lanzhou 730070, China. Tel: +86-13919449740, Email: sunw@gsau.edu.cn.

movement of the hole of the taking seed wheel, the characteristic size of the maize needs to be statistically counted and the shape needs to be classified. The experimental material was the Longdan No. 5 maize seeds (Gansu Academy of Agricultural Sciences, Crop Research Institute, and Gansu Long Yu Science and Technology Limited Liability Company selected). A total of 500 seeds were selected randomly, and their three-axis sizes are shown in Figure 1. A micrometer (accuracy 0.01 mm) was used to measure the height H , width W , and thickness T . Previous studies indicated that the head of the maize cob was in the form of a spherical cone, with a horse tooth in the central portion and with a spherical in the tail. However, most maize seeds were flat and irregular^[15]. For statistical convenience, the maize size can be expressed by the equivalent diameter. The equivalent diameter was calculated according to $D = \sqrt[3]{HWT}$, and its sphericity was estimated on $\phi = D/H$. Based on this, the maize was classified into 5 shape types, including horse tooth (sphericity: 0.57-0.66), spherical cone (sphericity: 0.63-0.77), spherical (sphericity: 0.77-0.96), oblate (sphericity: 0.80-0.85), and polygonal (sphericity: 0.91-0.93). According to the above classification, the number of horse tooth seeds accounted for 39.7% of the total, 42.7% for spherical cones, 8.7% for spherical, and a total of 8.9% for flat and polygonal shape seeds, the number ratio is shown in Figure 2. Only horse teeth, spherical cones, and spherical shape seeds are further analyzed and investigated conveniently their effect on seed metering performance. The formula ($V=HWT$) is used to calculate the volume, in turn, predict the volume distribution. All maize volume of the three shape types follows the normal distribution,

with standard deviation values of 0.092, 0.115, and 0.149 for the horse tooth, spherical cone, and spherical shape, respectively. The average dimensions are listed in Table 1. To improve the efficiency of the simulation, the maize model built in this study is a simplified model in contrast to the fine maize models^[16,17]. Also, to improve the reliability of the simulation model, the coefficient of rolling friction needs to be calibrated for different shape types^[14]. Maize models were established in the EDEM software (2018), as shown in Figure 3.

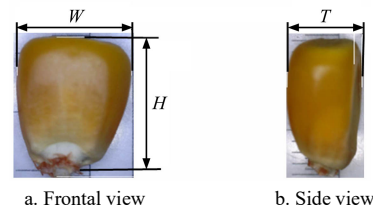


Figure 1 Characteristic size of maize

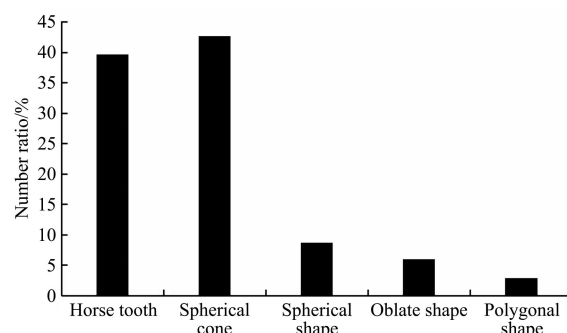


Figure 2 Number ratio for five shape types of maize seeds

Table 1 Diameter and sphericity of the maize varieties

Maize shape type	Average height H	Average width W	Average thickness T	Equivalent diameter D	Sphericity ϕ
Horse tooth	13.12	8.66	4.61	8.07	0.62
Spherical cone	11.37	7.15	5.86	7.81	0.69
Spherical	8.48	7.24	6.53	7.37	0.87

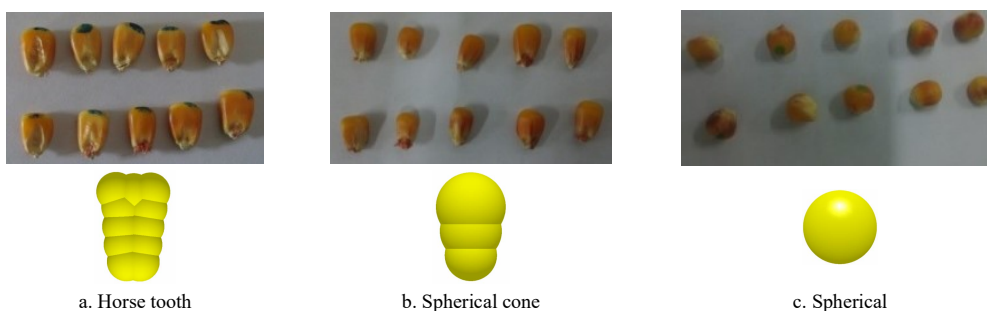


Figure 3 DEM maize simplified models

2.2 Seed metering device

A commercially available maize seed metering device with a high-filling-rate wheel was used in this study. It primarily consisted of a seed box, taking seed wheel, brushing seed wheel, disturbing seed wheel, etc., as shown in Figure 3a. The diameter of the taking seed wheel is 98 mm, and there are 16 eyelets along its circular direction, as shown in Figure 3b. The seed metering processes are classified into seed filling, seed disturbing and seed cleaning, seed transporting, seed metering. The seed filling rate affects the seed metering performance and is the most critical step. The inner shape and size of the eyelet hole are crucial to the filling of the seeds. The seed filling process is further classified into 3 types, namely extrusion filling, seed filling under gravity, and seed filling with disturbance. The structural size of the eyelets is shown in

Figure 3c. The front plate of the seed box is made of plexiglass for easily observing the seed motion, while the other plate is made of steel. The brushing seed wheel is a brush, and the taking seed and disturbing seed wheels are POM plastic. These wheels rotate in the counterclockwise direction. The contact models between the maize seeds and the seed metering device were selected as Hertz-Mindlin^[18]. The simulation time step percentage and grid size were fixed at 30% and $3R_{min}$, respectively^[19]. A total of 907 maize seeds were generated with the horse tooth, spherical cone, and spherical seed on the ratio of 18:19:4 in the seed box. The DEM model for metering seeds is shown in Figure 3d. Three detection areas in the seed box and three detection areas in taking seed wheel have been divided to study the motion of seeds, as shown in Figure 3e.

The angular speed of the taking seed wheel was calculated by

Equation (1)^[20]. The cavity distance was chosen as 220 mm. The minimum and maximum angular speeds corresponding to the minimum and maximum tractor speeds of 0.60 m/s and 2.83 m/s are 1.14 rad/s and 5.35 rad/s, respectively. The median value of 3.25 rad/s was also considered.

$$\omega = \frac{2\pi v}{am(1-\delta)} \quad (1)$$

where, v is the tractor speed, m/s; a is the cavity distance, m; m is the number of eyelets (here it is 16); δ is the ground wheel slip rate (here it is 5.7%)^[21].

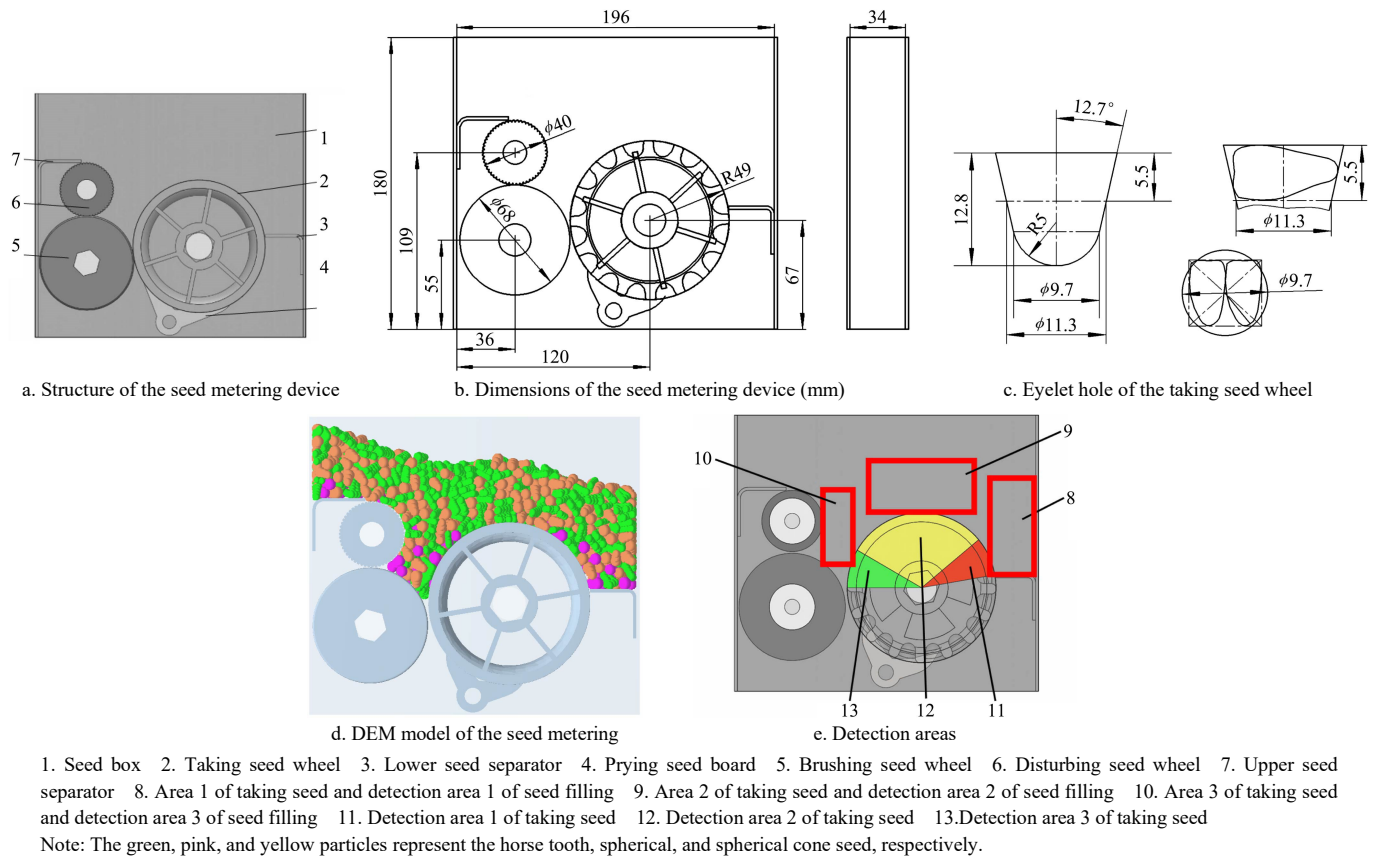


Figure 4 Simulation model of the seed metering device with a high-filling rate

2.3 Simulation parameters

The Hertz-Mindlin model includes some intrinsic and contact parameters. The intrinsic parameters consisted of the particle shape, size, volume distribution, center of mass location, mass density, bulk density, Poisson's ratio, elastic modulus, etc. Poisson's ratio and the elastic modulus are 0.4^[22] and 216.6 MPa^[23], respectively. The density obtained by the experiment is 1253.3 kg/m³. The maize moisture content varied from 10.75% to 11.33%, which was less than that 13%^[24]. Therefore, the Hertz-Mindlin model is appropriate. The contact parameters include the recovery coefficient, static friction, and rolling friction. The coefficient of static friction is 0.2^[25], and the recovery coefficient is 0.182^[12]. Although the uniformly calibrated coefficient of rolling friction regardless of its shape is basically the same as the actual repose angle, there are inconsistencies between the simulation and actual process in the kinetic and potential energy transformation during maize seeds flow.

Differences in gravity center and irregular shape of maize seed can affect the flow properties. However, it was reduced by adjusting the coefficient of rolling friction of maize models^[13,14,25,26]. Different seed shapes affect seed rolling behavior, requiring different coefficients of rolling friction. Maize seeds are classified by shape as horsetail, spherical cone, and spherical and differ greatly. Thus, the maize coefficient of rolling friction will be predicted separately to get an accurate result. Two containers were used to assist in the formation of the maize repose

angle. An aluminum cylinder container with an inner diameter of 54 mm and a height of 300 mm was lifted at a speed of 20 mm/s. The Plexiglas container, which had a length, width, and height of 100 mm, 60 mm, and 110 mm, respectively, was also lifted upwards at a speed of 20 mm/s. The actual repose angles of the horse tooth, spherical, spherical, horse tooth and spherical, spherical cone and spherical, and horse tooth and spherical cone shape types are 19.61°, 18.80°, 16.82°, 18.11°, 20.06°, and 23.67°, respectively. The relationship between the simulated repose angle and the coefficient of rolling friction for the horse tooth, spherical cone, spherical, horse tooth and spherical, spherical, and spherical, and horse tooth and spherical cone shape types were established by adjusting the coefficients of the rolling friction to obtain the same repose angle, as shown in Figure 5.

From Figure 5, the coefficient of rolling friction for the horse tooth, spherical cone, spherical, horse tooth and spherical, spherical cone and spherical, and horse tooth and the spherical cone is 0.018, 0.051, 0.105, 0.023, 0.177, and 0.068, respectively. Other parameters used in the seed metering simulation are shown in Table 2.

3 Results and discussion

The impact of the angular speed of the taking seed wheel on the maize seed transport and velocity in the seed box was investigated. Its effect on the seed filling, the seed metering performance, and the drop repose angle were also analyzed in detail.

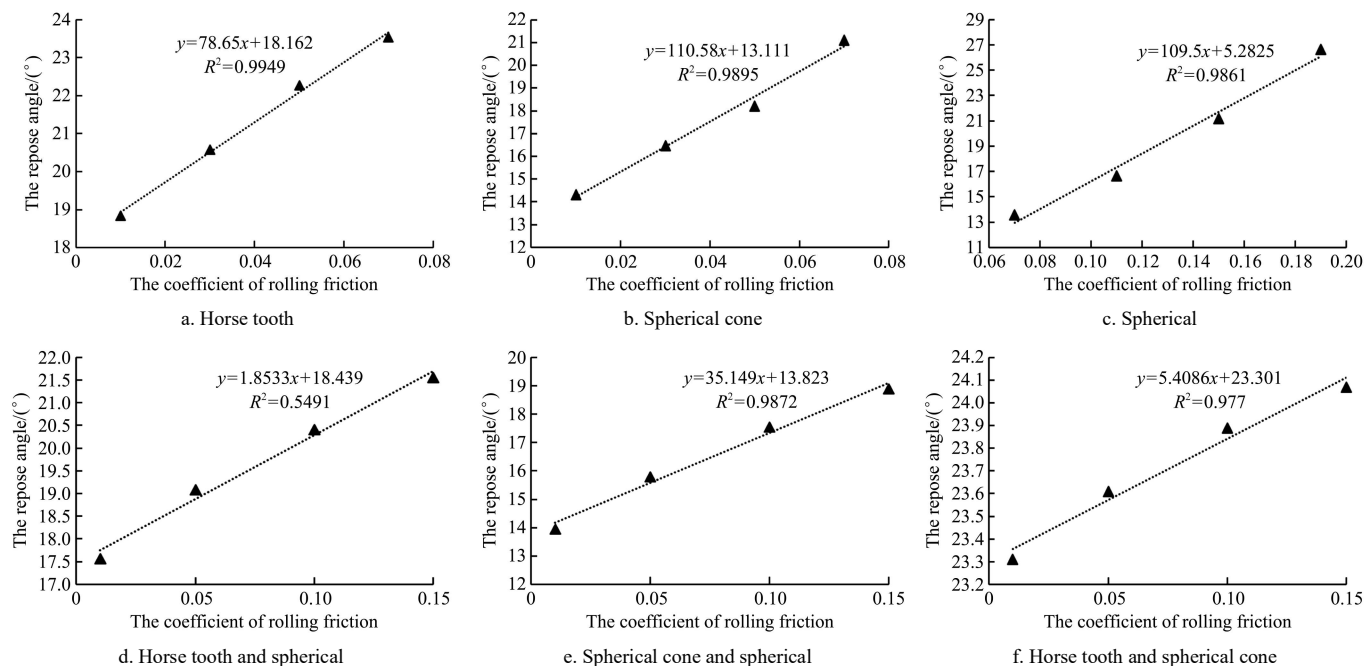


Figure 5 Relationship between the coefficient of rolling friction and the repose angle

Table 2 Simulation parameters

Parameters	Value	Reference
Poisson's ratio of plexiglass	0.35	[27]
Shear modulus of plexiglass/MPa	1.3×10^9	[27]
Density of plexiglass/kg·m ⁻³	1200	[27]
Recovery coefficient between the maize and plexiglass	0.621	[27]
Coefficient of static friction between the maize and plexiglass	0.459	[27]
Coefficient of rolling friction between the maize and plexiglass	0.0931	[27]
Poisson's ratio of aluminum	0.34	[14]
Shear modulus of aluminum/MPa	2.5×10^{10}	[14]
Density of aluminum/kg·m ⁻³	2.70	[14]
Recovery coefficient between the maize and aluminum	0.621	[28]
Coefficient of static friction between the maize and aluminum	0.342	[28]
Coefficient of rolling friction between the maize and aluminum	0.515	[28]
Poisson's ratio of POM plastic	0.4	EDEM
Shear modulus of POM plastic/MPa	1.0×10^6	EDEM
Density of POM plastic/kg·m ⁻³	1500	EDEM
Recovery coefficient between the maize and POM plastic	0.133	[21]
Coefficient of static friction between the maize and POM plastic	0.517	[21]
Coefficient of rolling friction between the maize and POM plastic	0.01	[21]
Density of brush/kg·m ⁻³	1150	[22]
Shear modulus of brush/MPa	100	[22]
Poisson's ratio of brush	0.4	[22]
Recovery coefficient between the maize and brush	0.3	[29]
Coefficient of static friction between the maize and brush	0.5	[29]
Coefficient of rolling friction between the maize and brush	0.3	[29]

3.1 Seed metering process

The seed metering simulation is shown in Figure 6. The specific seeding process is that the three wheels initiate seeds in the seed box transport, then a few maize seeds first fill the eyelets in the taking seed wheel, next the disturbing seed wheel further improves seeds activity in the disturbance filling area, in the following, the brushing seed wheel clears the excess seed in the eyelets, and the taking seed wheel metering the seed sequentially. Finally, the seeds that drop on the base plate form a drop repose angle. Seed filling the eyelets has three forms (Figure 7).

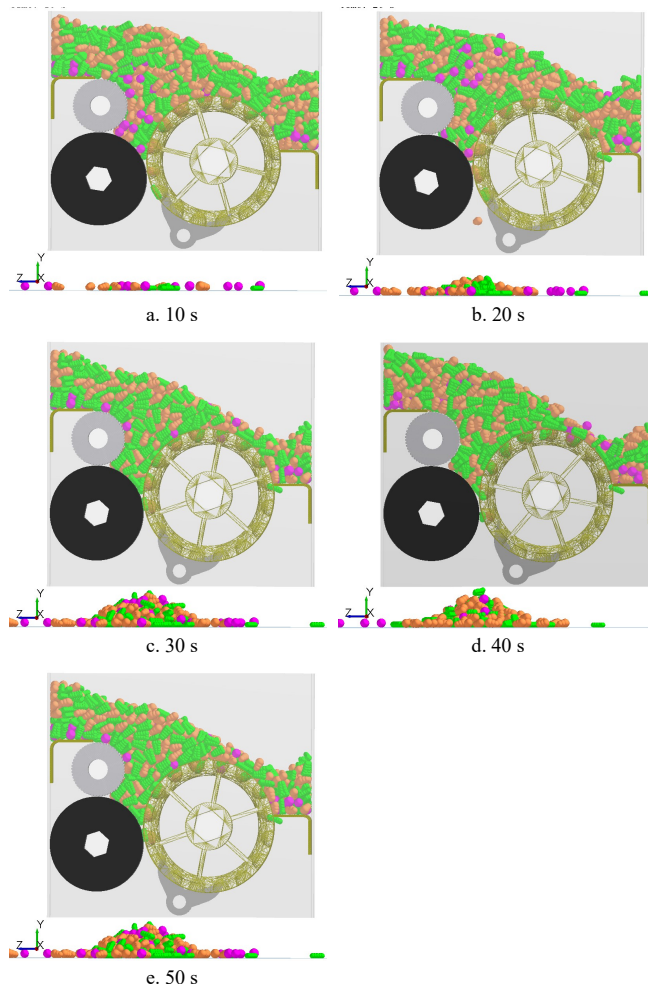


Figure 6 Maize seeds metering process

From Figure 7a, it was observed that maize seeds with relatively high velocities were in detection areas 2 and 3. The velocities of maize seeds in the eyelets were higher than those around the surface of the taking seed wheel, as shown in Figure 7b. From Figure 8c, it can be known that the direction of seeds movement in detection area 2 is tangential to the wheel rotation, at

this time some seeds that are in a loose position fall into the eyelets by gravity. From Figure 7d, it can be seen that the seeds enter the eyelets due to the crowding pressure exerted by the surrounding seeds. The above analysis demonstrates that the angular speed of the taking seed wheel influences the seed movement.

3.2 Effect of the angular speed of the taking seed wheel on seed movement in the seed box

The taking seed wheel brings the seed population transport. Its angular speed is an important parameter improving the seed-filling performance. Therefore, it is necessary to investigate the effects of the taking seed wheel and brushing seed wheel on seed transport in the seed box, as shown in Figure 8.

Figure 8 demonstrates that the rising angular speed of the taking seed wheel can increase the instantaneous seed average velocity, angular speed, and fluctuation amplitudes, enabling seed filling ability into the eyelets. Meanwhile, the seed filling performance also depends on the seed population transport cycle. The seeds vectors and the magnitude of the velocity are shown in Figure 9.

From Figure 9, it can be known that the taking seed wheel, brushing seed wheel, and disturbing seed wheel simultaneously drive seeds forming a small and large flow cycle. The small cycle is between the three wheels. Most seeds flow from right to left due to the rotation of the taking seed wheel, while the disturbing seed wheel brings nearby seeds upwards. Thus, seeds on the left side were higher than that on the right, and seeds further collapsed and slide into the right, this is the seed population large cycle. The decreasing number of maize seeds highlighted this trend. If the angular speed is 5.35 rad/s and the other wheels are 10.7 rad/s, the seed transport speed becomes significantly higher than those corresponding to angular speeds of 3.25 rad/s and 1.14 rad/s. The movement of the small and large seed population cycle accelerated simultaneously, thereby improving the efficiency of seed filling. Further, the effect of the angular speed on the different shapes of seed transport and speeds needs to be explored, as shown in Figure 10.

From Figure 10, it can be known that the horse tooth and spherical cone seeds were primarily located on the upper left of the

taking seed wheel. However, the spherical model was observed on both sides of the taking seed wheel. Since the contact area between the horse tooth and spherical cone seeds and the three wheels are relatively large, the seed velocities are higher than the spherical seeds and they were mainly involved in the large and small maize population, while the spherical cone seeds mainly were only in the small cycle. Around 50 s, the seed population was concentrated on the left, and the filling process was completed using gravity and disturbances forms.

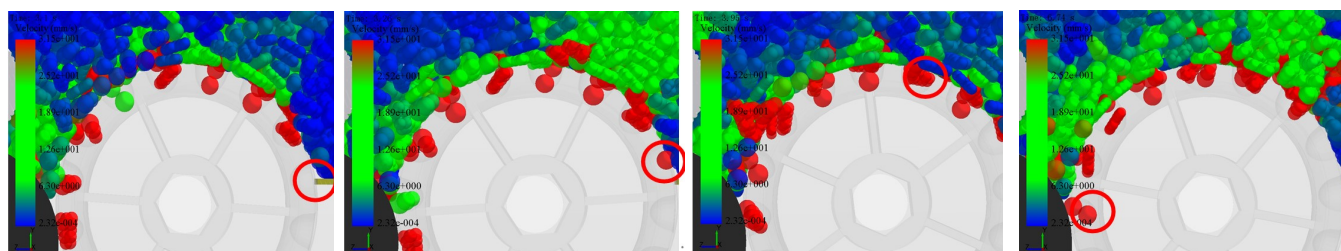
3.3 Effect of angular speed of taking seed wheel on seed filling in eyelets

Three detection areas were established in the taking seed wheel to study the seed filling in eyelets. Figure 11 shows the number of seeds filling.

From Figure 11, it can be known that the angular speed of the taking seed wheel influences the filling seed rate. Although detection area 2 includes five eyelets, the average number of seeds filling the eyelet was greater than five, implying that some eyelets were filled with two or more. In the detection area, 3 excess seeds were cleaned and the missing seed eyelets were filled. From Figure 11d, it can be found that the increasing angular speed gradually reduces the number of seeds in detection area 2. Due to the reduced number of seeds, the influence on detection area 1 is small. This demonstrates that the spherical seed acts as a lubricant in the population in deep, and its existence is conducive for seed filling.

The following parts specifically analyze the impact of the angular speed of the taking seed wheel on the taking seeds processes in areas 2 and 3, as shown in Figure 12.

From Figure 12, it can be known that the effect of the variability of the angular speed of the taking seed wheel on the different seed shape types is not obvious. The fluctuation range of the seed-taking number was significantly higher at an angular speed of 1.14 rad/s than those at 3.25 rad/s and 5.35 rad/s. The range stabilizes at an angular speed of 5.35 rad/s. With the increasing angular speed, the average number of seeds taking decreases for all shape types. This trend is consistent with that of the total number of seeds.



Note: The color of the maize changes from blue to red, and the speed increases, with green representing a value that lies between the low and high-speed values.

Figure 7 Seed filling forms

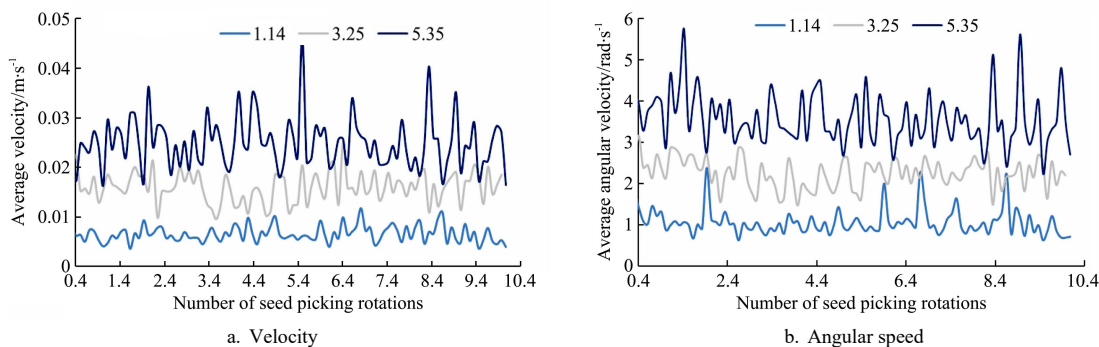


Figure 8 Velocity and angular speed of the maize seed in the seed box

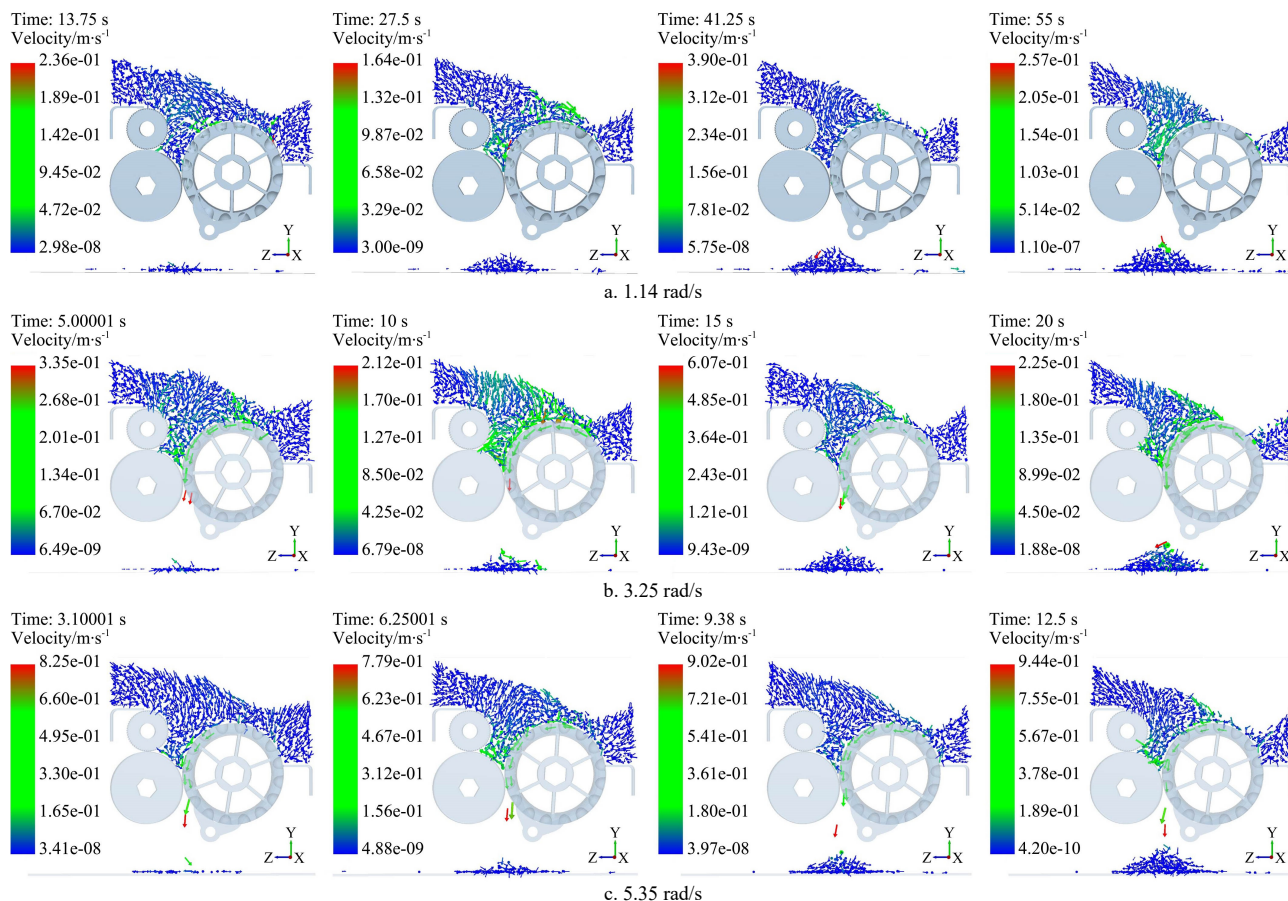


Figure 9 Seed population transport cycle in the seed box

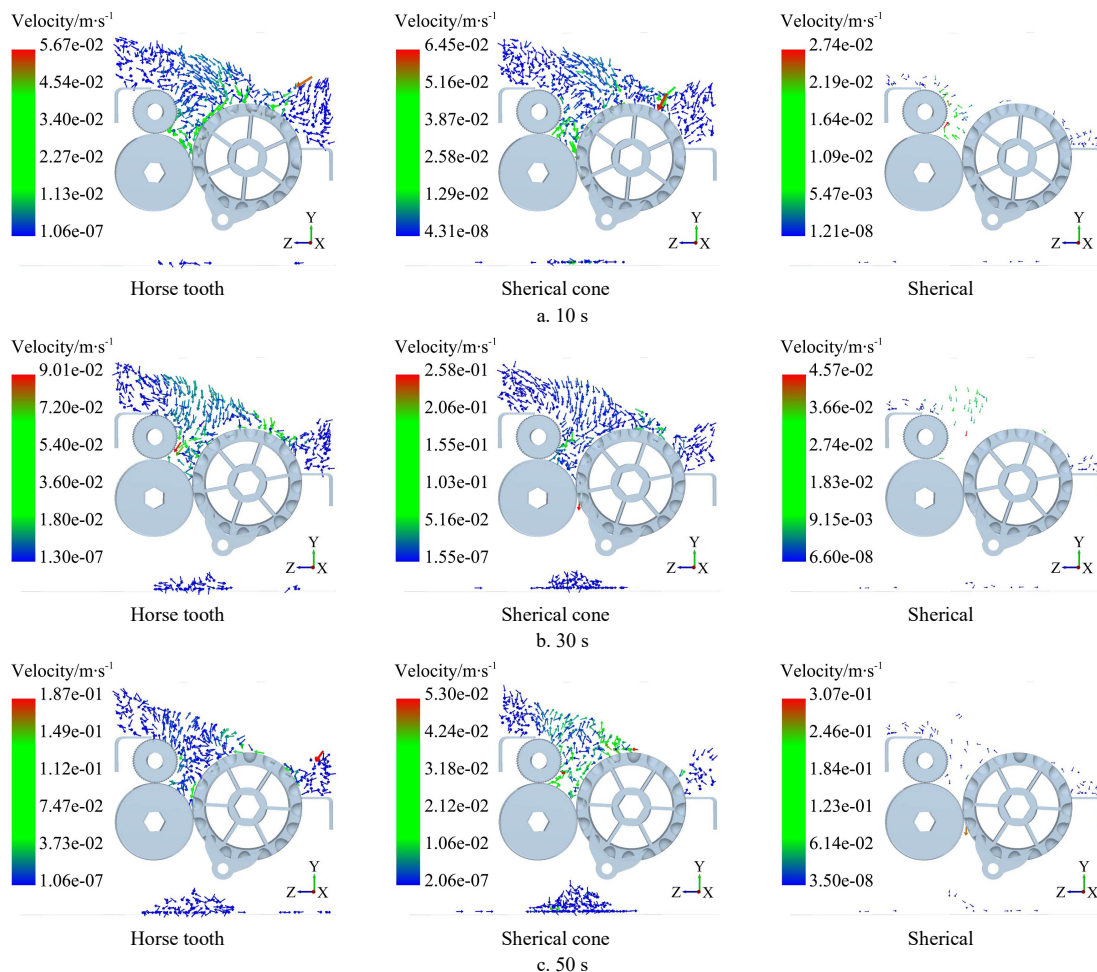


Figure 10 Seed transport and velocity in the seed box

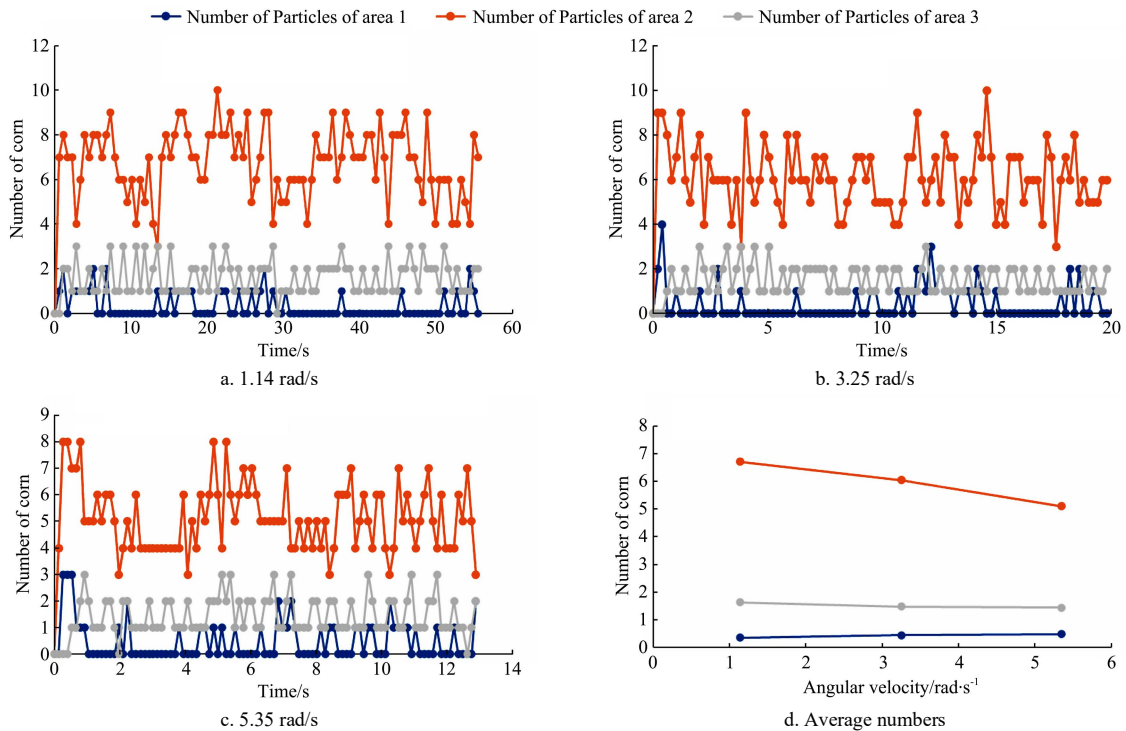


Figure 11 Effect of the angular speed of the taking seed wheel on the seed filling

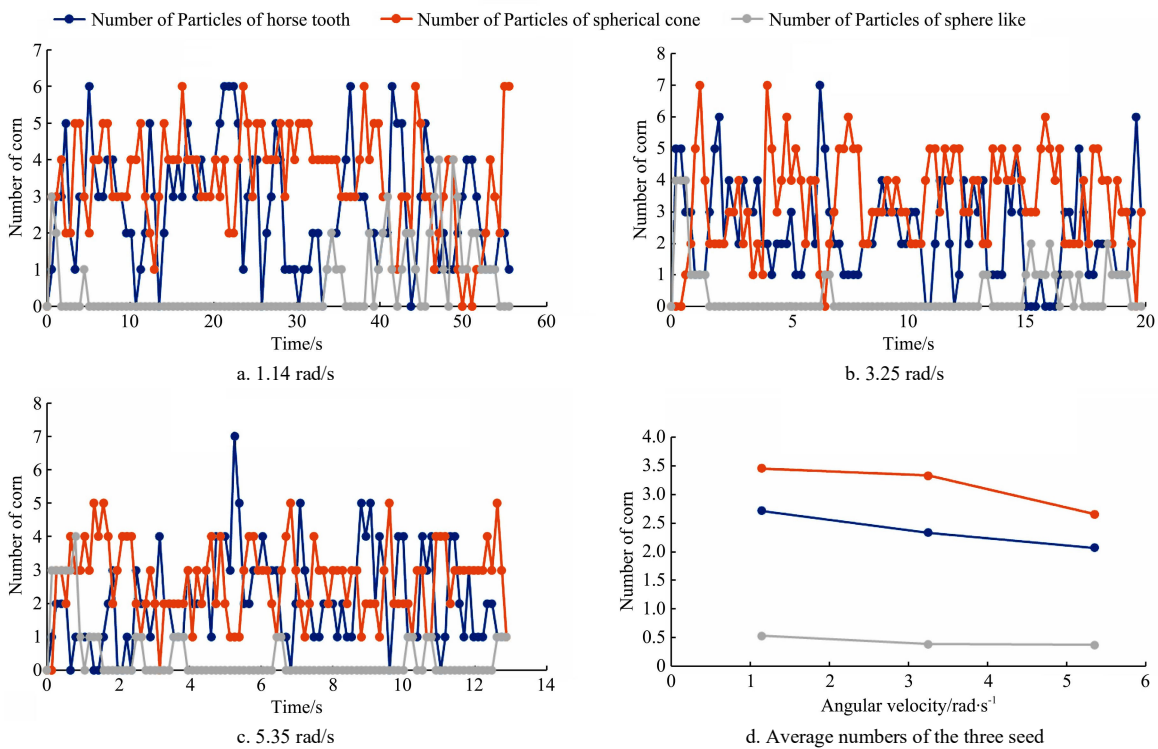


Figure 12 Effect of the angular speed of the taking seed wheel on the three shape types in detection area 2

3.4 Effect of the angular speed of the taking seed wheel on seed metering

The above analysis demonstrates that the angular speed of the taking seed wheel significantly affects the seed population movement. To examine the effect of the taking seed wheel speed on seed metering performance, the metering seed number under 3 angular speeds was compared, as shown in Figure 13.

Figure 13 demonstrates that the number of metering seeds number at a relatively low angular speed is higher than that at a relatively high speed. However, these differences are not obvious. The seed number was maximum for the spherical seeds and minimum for the spherical cone seeds.

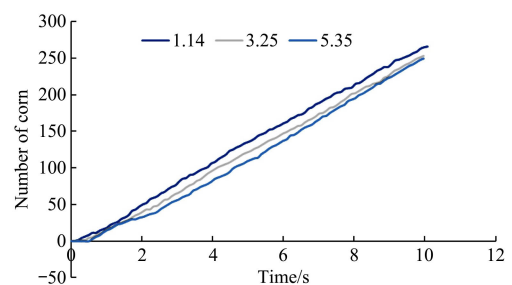


Figure 13 Variation of the seed metering number

To investigate the effect of the angular speed of the taking seed wheel on the metering performance, the transient variation of the

seed number with different angular speeds is shown in Figure 14.

Figure 14 indicates that the seed number was maximum and minimum for the spherical cone and spherical shape seeds, respectively. The increasing angular speed did not change this trend. Thus, the angular speed did not affect the seed metering significantly. The seed number of the spherical seed remained constant across different angular speeds. The seed numbers of the horse tooth and spherical cone seed increased, indicating that the overall metering performance of the irregular seed is superior to

that of the spherical seed. The effect of the angular speed on the variation of the seed number was further investigated by calculating the ratio of the seed number of the horse tooth model to that of the spherical cone seed. From Figure 14d, it can be known that the initial ratio of 0.93 decreases to approximately 0.65 at an angular speed of 1.14 rad/s, indicating that the metering velocity of the spherical cone changes rapidly. Following that, the ratio increases gradually and maintains a constant value of approximately 0.75.

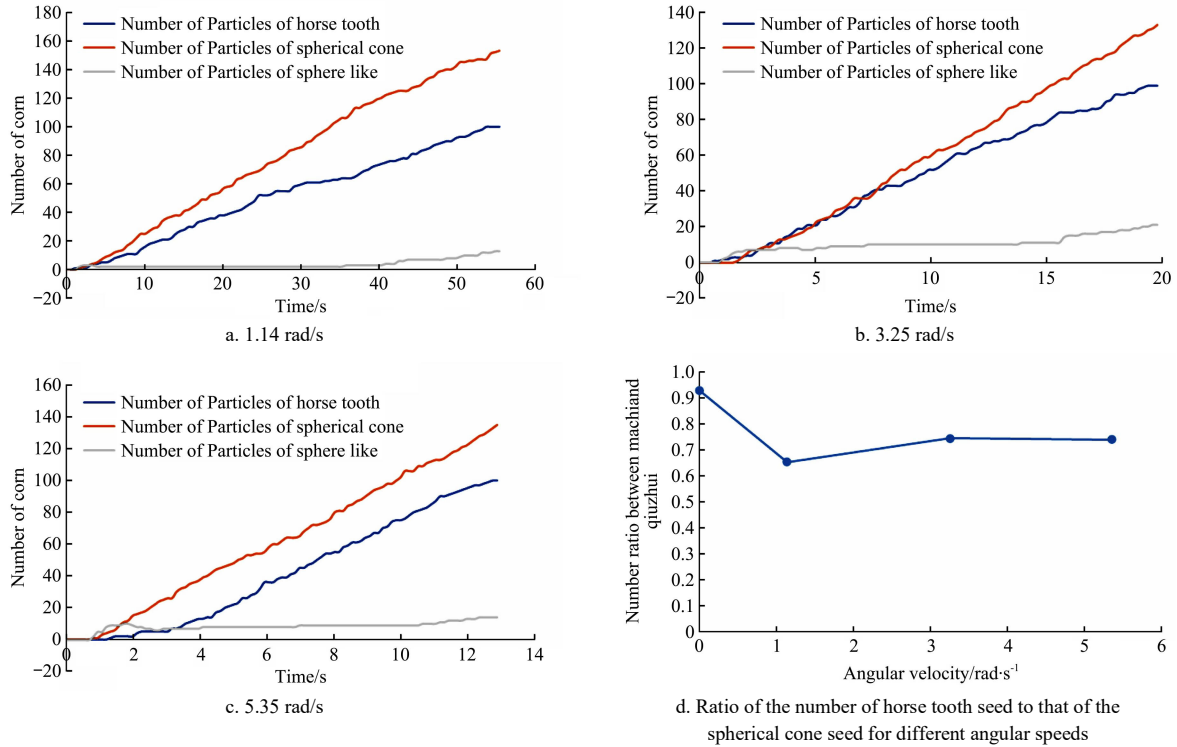


Figure 14 Transient variation of the seed number of the three shape types

3.5 Effect of the angular speed and maize shape on the drop repose angle

The maize repose angle is a macroscopic characterization of seed flow. The repose angle is relatively large for seed with difficult flow and relatively small for smooth-flowing seeds. The variation of the maize repose angle was analyzed to explore the

effect of the angular speed on the repose angle, as shown in Figure 15. The repose angle at angular speeds of 1.14, 3.25, and 5.35 rad/s is 26.58°, 27.06°, and 27.13°, respectively. In addition, the effect of the seed shape on the repose angle was also analyzed by comparing the maize repose angle at constant angular speeds of the taking seed wheel.

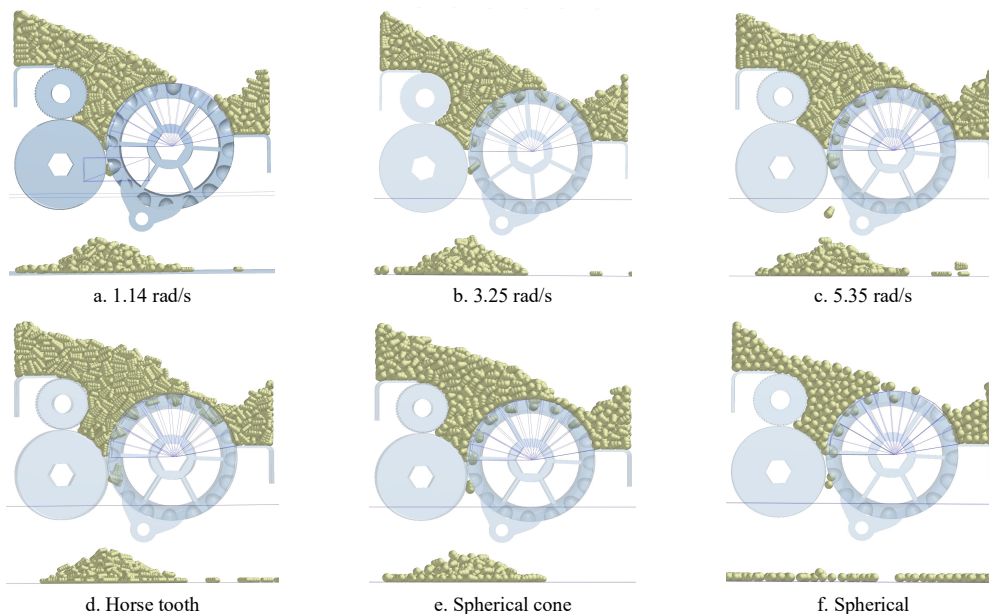


Figure 15 Effect of the angular speed of the taking seed wheel and maize shape on the maize repose angle

From Figure 15, it can be known that the repose angle gradually with the angular speed increasing, but this variation was not obvious. The drop range at an angular speed of 1.14 rad/s is greater than those at angular speeds of 3.25 rad/s and 5.35 rad/s. In addition, the repose angle of the horse tooth seed is larger than that of spherical cone and spherical seed. This indicates that the irregular maize can reduce the coefficient of variation of plant spacing between seeds, which is useful to improve the quality of metering.

4 Verification

The accuracy of the metering seed simulations was verified through experiments conducted in March 2020. 907 maize seeds (Longdan No. 5) were selected such that the ratio of the horse tooth, spherical cone, and spherical models was 18: 19: 4. They were marked with different colors and poured into the seed box of the metering seed device after approximately one minute of mixing. An adjustable-speed motor (PC MOTOR, Suzhou Haoyuan Mechanical & Electrical Co., Ltd) was used to drive the seed metering device (4-430 r/min). Angular speeds of 1.14 rad/s (speed I), 3.25 rad/s (speed II), and 5.35 rad/s (speed III) were used

for the seed taking wheel, while those of the brushing seed wheel and disturbing seed wheel were twice that of the seed taking wheel in the same direction. Ten revolutions of the seed taking wheel were assessed to determine the metering performance, which corresponds to experiment durations of 55 s, 19 s, and 11 s for speeds I, II, and III, respectively. The number of metering seeds was recorded during the process. The metering seed device is shown in Figure 16. A comparison between the number of the taking seed obtained through simulations and experiments is shown in Figure 17.



Figure 16 Metering seed device

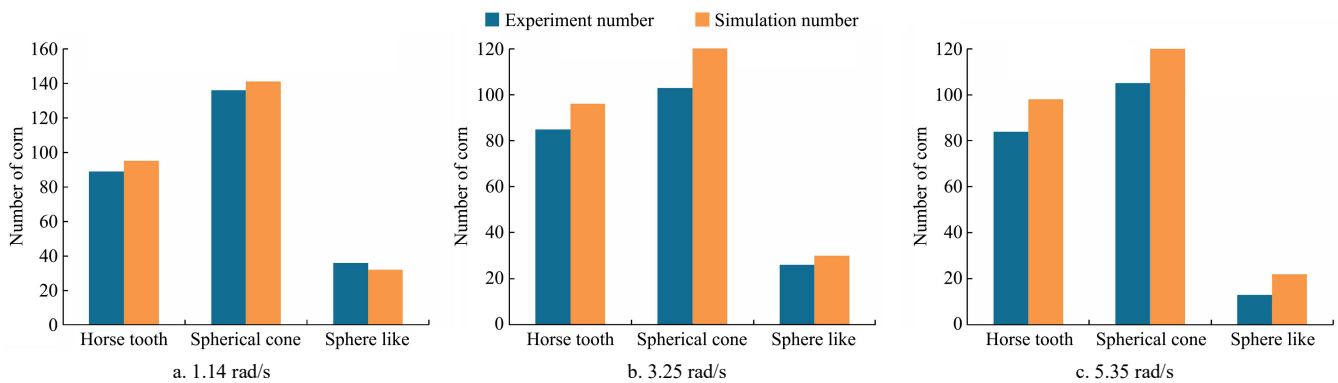


Figure 17 Comparison between maize metering number obtained through simulation and experiment

From Figure 17, the relative errors of the metering number for the horse tooth, spherical cone, and spherical seeds between simulation and experiment are 6.74%, 3.55%, and 11.11% at 1.14 rad/s, 11.46%, 8.04%, and 7.69% at 3.25 rad/s, and 5.95%, 4.76%, and 13.33% at 5.35 rad/s, respectively.

The simulating and experimental metering rates of the single and multiple seeds were compared. According to the GB/T 6973-2005 single grain (precision) seeder experiment method, the single seed rate S and multi-seed rate D were determined by Equations (2) and (3). The results of the simulation and experiment are shown in Table 3.

$$S = \frac{n_1}{N} \times 100\% \quad (2)$$

$$D = \frac{n_2}{N} \times 100\% \quad (3)$$

where, N is the theoretical number of metering seeds; n_1 is the number of single seeds, and n_2 is the number of multiple seeds.

Table 3 shows that when the angular speed of the taking seed wheel is 1.14 rad/s, the experimental single seed rate was 78.54%, and the relative error between the experiment and simulation result was 2.28%. When the angular speed of the taking seed wheel is 3.25 rad/s, the experiment single seed rate was 71.88%, and their relative error was 2.76%. When the angular speed of the taking seed wheel is 5.35 rad/s, the experiment single seed rate was 85.22%, and their relative error was 1.56%. Also, their multi-seed

rate errors not exceeding 10%. Therefore, the single-seed and multi-seed rate are basically similar between the simulation and the experiment at the three angular speeds of the taking seed wheel.

Table 3 Comparison between the simulating and experimental number of seed metering

The angular speed of the taking seed wheel/rad·s ⁻¹	Index	Index	
		Single seed rate/%	Multi-seed rate/%
1.14	Experiment	78.54	21.46
	Simulation	80.37	19.63
3.25	Experiment	71.88	28.12
	Simulation	73.92	26.08
5.35	Experiment	85.22	14.78
	Simulation	86.55	13.45

5 Conclusions

1) The simulation of seed metering device with a high-filling rate was conducted to explore the effects of the taking seed wheel on the movement of the seed population in the seed box. In addition, the taking and metering seed and their repose angles were also investigated in detail.

2) It was observed that the seed in the seed box formed small and large circles due to the disturbances caused by the three wheels. A rise in the angular speed of the three wheels can significantly improve the seed transport velocity and angular speed and yet reduce the rate of seed filling in the seed filling regions. The

change in the angular speed of the taking seed wheel did not impact the selection of the seed shape significantly; however, the taking seed rate decreased for the horse tooth and spherical cone seeds. Moreover, a rise in the angular speed did not affect the taking seed numbers significantly.

3) The repose angle formed by the seed drop for varying angular speeds was also analyzed. The angular speed of the taking seed wheel affected the repose angle. The increasing angular speed reduced the coefficient of variation of the seed drop. In addition, the repose angle of the horse tooth seed was greater than that of the spherical cone and spherical seeds. Thus, irregular seeds can also reduce the coefficient of variation of the seed drop. Also, the experimental and simulated results were similar in terms of the number of metering seeds. The reliability of the proposed calibration method for the maize coefficient of rolling friction was further verified by the metering seed experiment.

Acknowledgements

This work was financially supported by the National Natural Science Foundation of China (Grant No. 52065004, 52165028), and Special Talent of Gansu Agricultural University (Grant No. GAU-KYQD-2020-15, GAU-KYQD-2020-33).

[References]

- [1] Li H. Digital design and simulation analysis of working process for the precision seed-metering device. Master dissertation. Changchun: Jilin University, 2004; 48p. (in Chinese)
- [2] Chen J, Zhou H, Zhao Z, Li Y M, Gong Z Q. Analysis of rice seeds motion on vibrating plate using EDEM. Transactions of the CSAM, 2011; 42(10): 79–83, 100. (in Chinese)
- [3] Chen Y, Hu Z C, Wu H C, Wang S Y, You Z Y. Simulation research on sampling mechanism of single resistance typed grain on-line moisture teller based on EDEM. Transactions of the CSAM, 2016; 38(7): 239–244, 262. (in Chinese)
- [4] Coetzee C J, Els D. Calibration of discrete element parameters and the modelling of silo discharge and bucket filling. Computers & Electronics in Agriculture, 2009; 65(2): 198–212.
- [5] He T, Jin B S, Zhong W Q, Wang X F, Ren B, Zhang Y, et al. Discrete element method modeling of non-spherical granular flow in rectangular hopper. Chemical Engineering & Processing Process Intensification, 2010; 49(2): 151–158.
- [6] Wensrich C M, Katterfeld A. Rolling friction as a technique for modelling particle shape in DEM. Powder Technology, 2012; 217: 409–417.
- [7] Combarros M, Feise H J, Zetzener H, Kwade A. Segregation of particulate solids: Experiments and DEM simulations. Particuology, 2014; 12: 25–32.
- [8] Han Y L, Jia F G, Tang Y R, Liu Y, Zhang Q. Influence of granular coefficient of rolling friction on accumulation characteristics. Acta Physica Sinica - Chinese Edition, 2014; 63(17): 173–179. (in Chinese)
- [9] Wang Z C. A mechanism of rolling friction and the coefficient of rolling friction. J. Shanghai Inst. Mech. Eng., 1993; 15(4): 35–43. (in Chinese)
- [10] Jia F G, Han Y L, Liu Y, Cao Y P, Shi F F, Yao L N, et al. Simulation prediction method of repose angle for rice particle materials. Transactions of the CSAE, 2014; 30(11): 254–260. (in Chinese)
- [11] Yan H. A new kind of method for the optimized design of combination inner-cell corn precision seed metering device. Doctoral dissertation. Changchun: Jilin University, 2012; 178p. (in Chinese)
- [12] Wang Y X, Liang Z J, Zhang D X, Cui T, Shi S, Li K H, et al. Calibration method of contact characteristic parameters for corn seeds based on EDEM. Transactions of the CSAE, 2016; 32(22): 36–42. (in Chinese)
- [13] Wu H L, Cui T, Fan C L, Zhao H H, Du Y T. Study on the effect of maize seed gravity center on the performance of metering device. In 2019 ASABE Annual International Meeting, Boston, Massachusetts, 2019; Paper No. 1900731. doi: 10.13031/aim.201900731.
- [14] Shi L R, Zhao W Y, Sun B G, Sun W. Determination of the coefficient of rolling friction of irregularly shaped maize particles by using discrete element method. Int J Agric & Biol Eng, 2020; 13(2): 15–25.
- [15] Wang L J, Zhou W Q, Ding Z J, Li X X, Zhang C G. Experimental determination of parameter effects on the coefficient of restitution of differently shaped maize in three-dimensions. Powder Technology, 2015; 284: 187–194.
- [16] Zhou L, Yu J Q, Wang Y, Yan D X, Yu Y J. A study on the modelling method of maize-seed particles based on the discrete element method. Powder Technology, 2020; 374: 353–376.
- [17] Zhou L, Yu J Q, Liang L S, Wang Y, Yu Y J, Yan D X, et al. DEM parameter calibration of maize seeds and the effect of rolling friction. Processes, 2021; 9(6): 914. doi: 10.3390/pr9060914.
- [18] Liao Q X, Zhang P L, Liao Y T, Yu J J, Cao X Y. Numerical simulation on seeding performance of centrifugal rape-seed metering device based on EDEM. Transactions of the CSAM, 2014; 45(2): 109–114. (in Chinese)
- [19] Chen Z R. An approach to and validation of maize-seed-assembly modeling based on the discrete element method. Master dissertation. Changchun: Jilin University, 2019; 119p. (in Chinese)
- [20] Hu G M. Analysis and simulation of granular system by Discrete element method using EDEM. Wuhan: Wuhan University of Technology Press, 2010; 302p. (in Chinese)
- [21] Li X F, Liu F, Zhao M Q, Zhang T, Li F L, Zhang Y. Determination of contact parameters of maize seed and seed metering device. Journal of Agricultural Mechanization Research, 2018; 40(10): 149–153. (in Chinese)
- [22] ASAE Standards. S368. 4DEC2000(R2006). Compression experiment of food materials of convex shape. St Joseph: ASABE, 2006.
- [23] Zhao W. Research on combined spiral plate tooth seed corn threshing device. Northwest Agriculture and Forestry University, 2012, pp.49–51. (in Chinese)
- [24] ASAE Standards S352.2-2003. Moisture measurement unground grain and seeds. ASAE, 2003.
- [25] Shi L R, Yang X P, Zhao W Y, Sun W, Wang G P, Sun B G. Investigation of interaction effect between static and rolling friction of corn kernels on repose formation by DEM. Int J Agric & Biol Eng, 2021; 14(5): 238–246.
- [26] Shi L R, Zhao W Y, Wu J M, Zhang F W, Sun W, Dai F, et al. Application of slice modeling technology in finite element analysis of agricultural products. Journal of Chinese Agricultural Mechanization, 2013; 34(3): 95–98. (in Chinese)
- [27] Cui T, Liu J, Yang L, Zhang D X, Zhang R, Lan W. Experiment and simulation of rolling friction characteristic of corn seed based on high-speed photography. Transactions of the CSAE, 2013; 29(15): 34–41. (in Chinese)
- [28] Shi S. Design and experimental research of the pneumatic maize precision seed-metering device with combined holes. Doctoral dissertation. Beijing: China Agricultural University, 2015; 132p. (in Chinese)
- [29] Shi L R, Wu J M, Sun W, Zhang F W, Sun B G, Liu Q W, et al. Simulation test for metering process of horizontal disc precision metering device based on discrete element method. Transactions of the CSAE, 2014; 30(8): 40–48. (in Chinese)